



## Synergy of electrochemical and ozonation processes in industrial wastewater treatment

Lina A. Bernal-Martínez<sup>a</sup>, Carlos Barrera-Díaz<sup>a,\*</sup>, Carlos Solís-Morelos<sup>b</sup>, Reyna Natividad<sup>a</sup>

<sup>a</sup> Centro Conjunto de Investigación en Química Sustentable, UAEM-UNAM, Carretera Toluca-Atlaconulco, Km 14.5, Unidad El Rosedal, C.P. 50200, Toluca Estado de México, Mexico

<sup>b</sup> Centro Interamericano de Recursos del Agua, Carretera Toluca-Atlaconulco, Km 14.5, C.P. 50200, Toluca Estado de México, Mexico

### ARTICLE INFO

#### Article history:

Received 1 July 2010

Received in revised form 23 August 2010

Accepted 24 August 2010

#### Keywords:

Effluent

Electrochemical

Ozone

COD

Integrated

### ABSTRACT

The effectiveness of electrochemical, ozone and integrated electrochemical–ozone processes on industrial wastewater was evaluated. Electrochemical under optimal conditions of pH 7 and  $40 \text{ mA cm}^{-2}$  of current density reduced the chemical oxygen demand (COD) by 43% and the biochemical oxygen demand (BOD<sub>5</sub>) by 42%. Ozone treatment reduced both COD and BOD<sub>5</sub> by 60%. Integration of the two processes at pH 7 and  $20 \text{ mA cm}^{-2}$  of current density greatly improved the reduction of COD (84%), BOD<sub>5</sub> (79%), color (95%), turbidity (96%) and total coliforms (99%). Thus, the integrated electrochemical–ozone process noticeably improves wastewater quality. Finally, the sludge produced during integrated electrochemical–ozone process was quantified and the morphology was evaluated by scanning electron microscopy (SEM) and energy dispersive X-ray analysis (EDX).

© 2010 Elsevier B.V. All rights reserved.

### 1. Introduction

Water quality and availability is a challenging problem facing societies all over the world [1]. Conventional biological, physical, and chemical methods of water and wastewater treatment have limited success when applied to the treatment of industrial effluents since wastewater contains stable refractory organic compounds. These processes also tend to generate large amounts of sludge, which require treatment before final disposal [2,3].

Recently, attention has focused on advanced oxidation processes (AOPs) to reduce the refractory organic pollutants in effluents [4–8]. AOPs are oxidation processes that generate hydroxyl radicals in sufficient quantity to affect chemical transformation of contaminants [9,10]. Particularly, AOPs have been reported as powerful technologies capable of degrading a wide variety of refractory compounds and as alternatives for the treatment of highly stable wastewater [11–13].

Ozone-based AOPs are much more efficient than ozone alone in the removal of persistent organic compounds in wastewater. These processes can completely oxidize recalcitrant compounds into biodegradable products [14–18]. The coupling of ozone with activated carbon [19], hydrogen peroxide and UV radiation [20] has been shown to improve the efficiency by opening the additional pathway of decomposition into hydroxyl radicals.

Certain combinations of AOPs like Fenton and photo-Fenton that involve the addition of iron into solution have been proposed to increase the capacity and degree of mineralization of refractory pollutants [21–23]. Fenton reagent generation, is typically most efficient in acidic solution, which requires the addition of more chemicals. Therefore, new ways to utilize iron and ozone together in mild pH conditions are needed. In this work, we investigated introducing iron ions during ozonation. In addition, we evaluated how the pH affects the efficiency of the process, the optimum ozone and iron doses, and the amount and quality of the sludge.

### 2. Materials and methods

#### 2.1. Wastewater samples

Samples of wastewater were collected from a treatment plant located at the end of an industrial park, which receives the discharge of 144 different facilities. The samples were collected in plastic containers and cooled down to  $4^\circ\text{C}$ , then transported to the laboratory for analysis and treatment. The quality parameters of the wastewater prior treatment (raw water) were: COD of  $410 \text{ mg L}^{-1}$ , color of 520 Pt–Co, turbidity of 55 NTU and pH of 7.5.

#### 2.2. Electrochemical reactor

A batch electrochemical reactor was constructed for the electrochemical step. The reactor cell contains an array of six parallel monopolar iron electrodes. Each electrode was 5.5 cm by 3.0 cm with a surface area of  $16.5 \text{ cm}^2$ . All together, the total anodic

\* Corresponding author. Tel.: +52 722 2173890; fax: +52 722 2175109.  
E-mail address: [cbd0044@yahoo.com](mailto:cbd0044@yahoo.com) (C. Barrera-Díaz).

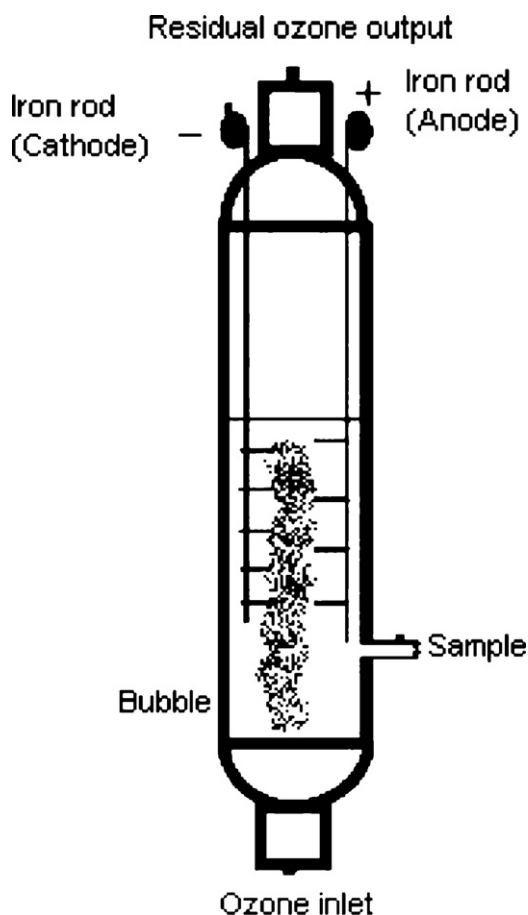


Fig. 1. Reactor representing the experimental set up of integrated electrochemical–ozone treatment systems.

surface ( $A_a$ ) was  $99 \text{ cm}^2$ . While the capacity of the reactor vessel was 1.5 L, 1.0 L was used in all of the trials. A direct-current power source supplied the system with 1–4 A, corresponding to current densities of  $10\text{--}40 \text{ mA cm}^{-2}$ , in keeping with previous work [24,25].

### 2.3. Ozone reactor

The ozone experiments were conducted in a 1.0 L glass reactor at  $18^\circ\text{C}$ . Ozone was supplied by a Pacific Ozone Technology generator. The gas was fed into the reactor through a porous plate situated at the reactor bottom. The ozone concentration at the gas inlet and outlet of the reactor was measured by redirecting the flows to a series of flasks containing 0.1 M potassium iodide [26]. The mean concentration of ozone in the gas phase was  $5 \pm 0.5 \text{ mg L}^{-1}$  and was measured immediately before each run. Ozonation experiments were carried out at pH 3, 5, 7 and 9, and samples were taken at regular intervals to measure COD, color and turbidity.

### 2.4. Integrated electrochemical–ozone process

Iron electrodes were installed in the ozone reactor as shown in Fig. 1. Ozone was introduced into the reactor with the iron electrodes at various current intensities. Experiments were carried out at pH 3, 5, 7 and 9, adjusting the pH (using NaOH or  $\text{H}_2\text{SO}_4$ ) with samples taken at regular intervals to measure COD, color and turbidity.

### 2.5. Methods of analysis

The initial evaluations of the electrochemical, ozonation and integrated treatments were determined by analysis of the COD ( $\text{mg L}^{-1}$ ), color (Pt–Co scale), and turbidity (NTU scale) at different pH values over time. However, once the optimal conditions were found the raw and treated wastewater samples were analyzed using the Standard Methods for the Examination of Water and Wastewater Procedures [27].

### 2.6. Sludge characterization

The sludge generated by the electrochemical treatment and by the integrated system was analyzed by scanning electron microscope (SEM) and energy dispersive X-ray microanalysis (EDX). The analysis was performed on a JEOL JSM-6510LV microscope to evaluate the features and morphology of the structure. SEM provides images of submicron features while energy dispersive X-ray analysis (OXFORD, INCApentaFETX3) offers *in situ* elemental analysis.

## 3. Results and discussion

### 3.1. Electrochemical treatment

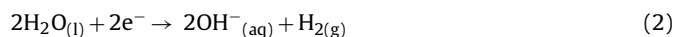
#### 3.1.1. Effect of pH

It is well known that the initial pH of the sample can have either a positive or negative influence on the electrochemical treatment performance. Hence, after the samples were introduced into the reactor, the pH was initially adjusted using either NaOH or  $\text{H}_2\text{SO}_4$  before the electrical current was applied. In our experiments, we used pH values of 3, 5, 7 and 9. The COD ( $\text{mg L}^{-1}$ ) as function of treatment time at different initial pH values is shown in Fig. 2A. The maximum COD reduction occurs at pH 7 (43%), followed closely by that at pH 9 (39%) after 20 min reaction time and that at pH 3 and 5 (36–37%) after 30 min reaction time. Based on a statistical analysis (*t*-test), these differences are considered not significant. On the contrary, pH does have an impact on COD removal rate and this may be due to pH role in significantly affecting rates of Eqs. (1) and (3) [28–30]. The former is favored by  $\text{pH} < 5$  [34], while the latter is evidently improved at basic pH. In this case, it is observed that the COD removal rate is highest at pH 7 and 9. This is evidenced by the time at which the maximum % removal is achieved ( $\sim 20$  min). Thus this time was selected to plot COD % removal as a function of pH (Fig. 2B). At this point of the reaction, the COD % removal reaches a maximum for initial pH 7 and 9 and the difference with that achieved in the acidic region is significant. This fact could be explained based on electrocoagulation mechanism and predominance zone diagrams for Fe(II) chemical species in aqueous solution. The electrocoagulation treatment of wastewater using iron electrodes takes place according to the following (Eqs. (1)–(4)) [31–35].

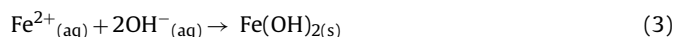
Anodic reaction:



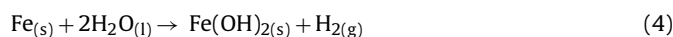
Cathodic reactions:



Solution reaction



Overall reaction:



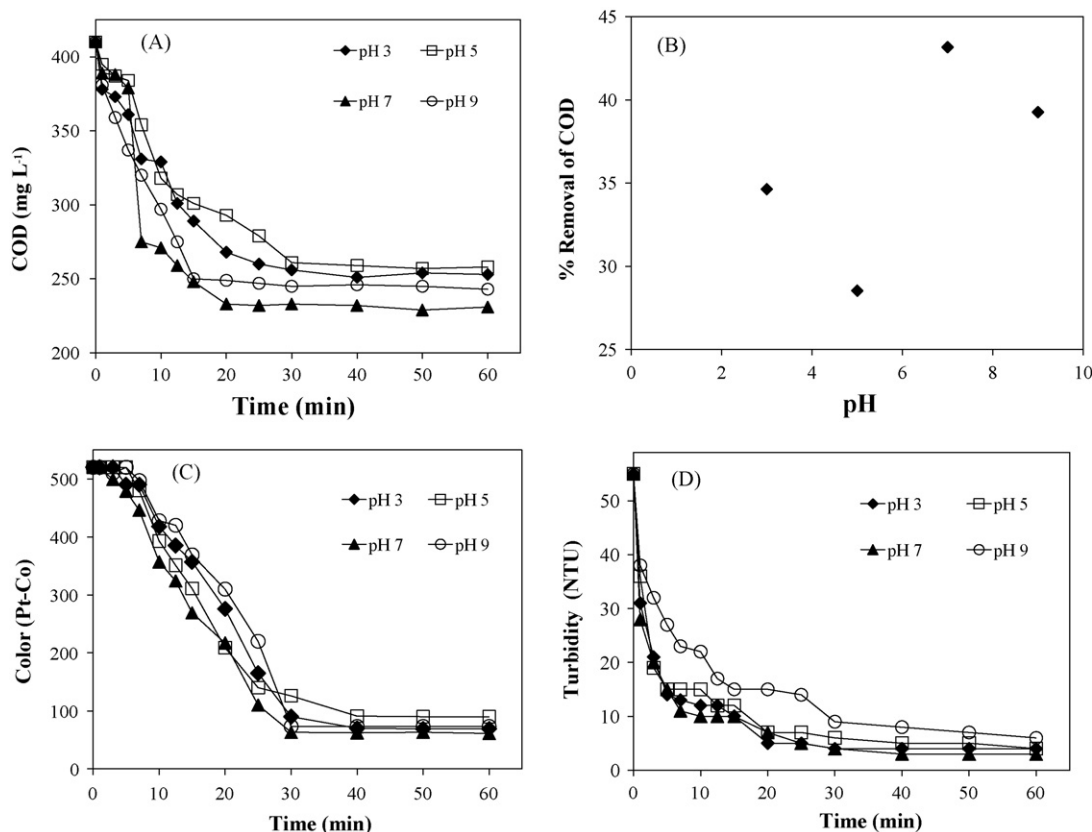


Fig. 2. Removal of (A) COD ( $\text{mg L}^{-1}$ ), (B) COD % removal as a function of pH, (C) color (Pt-Co) and (D) turbidity (NTU) from wastewater at different pH (3, 5, 7 and 9) as a function of electrochemical treatment time.

According to literature, Eq. (1) is favored at  $\text{pH} < 5.0$  because of the chemical attack of protons [34,36] and hence predominantly monomeric species like  $\text{Fe}^{2+}$  in solution can be expected. Because of Eq. (2) an increase in pH would be expected and would lead to the appearance of the insoluble floc in Eq. (3). This insoluble floc is able to remove contaminants either by surface complexation or electrostatic attraction [28]. In consequence, the reaction would be slower in the acidic region since it has to spend longer time into reaching the zone where all plausible complexing species co-exist (high pH) as shown in Fig. 2C. The flocs concentration is directly related to pH and this may explain why turbidity is higher at pH 9 (Fig. 2D). As illustrated in Fig. 2D, at pH 3, 5 and 7, the maximum removal of turbidity was similar ( $\sim 90\%$ ). However, due to a higher oxidation rate and the no need of electrocoagulation influent pH adjustment, pH 7 is the most advisable to carry out the electrocoagulation process of such a complex reacting solution. Coincidentally, the best pH range of electrocoagulation could also be beneficial to the ozone process.

### 3.1.2. Influence of applied current density

The COD as a function of treatment time for different applied current densities at pH 7 is shown in Fig. 3. As the applied current density was increased from 10 to  $40 \text{ mA cm}^{-2}$ , the COD removal did not rise significantly in the range of 20– $40 \text{ mA cm}^{-2}$ . This is ascribed to the fact that an increase in current density leads to an increase in the quantity of oxidized iron generated from the electrode (Eq. (1)). As expected, higher current densities produced larger reductions in COD. However, as the current density was increased, the applied potential also increased. Thus, it is advisable to limit the current density to avoid adverse effects such as heat generation. This result agrees with the findings reported by Panizza and coworkers [37–39].

## 3.2. Ozone

### 3.2.1. Effect of pH

We investigated the effect of pH (3, 5, 7 and 9) on COD, color and turbidity removal efficiency in a series of experiments using a concentration of  $5 \text{ mg L}^{-1}$  of ozone. The COD as a function of treatment time for different pH values is shown in Fig. 4A. There can be distinguished three different kinetic stages in the profiles depicted in Fig. 4A, at pH 3–7. It is evident that during the first one (0–5 min), a faster oxidation takes place (given by COD diminishment rate) than the one observed in the range of 5–15 and 15–60 min of treatment. This phenomenon may be ascribed to the complexity of the reacting solution, which is a mixture of effluents of several industries (phar-

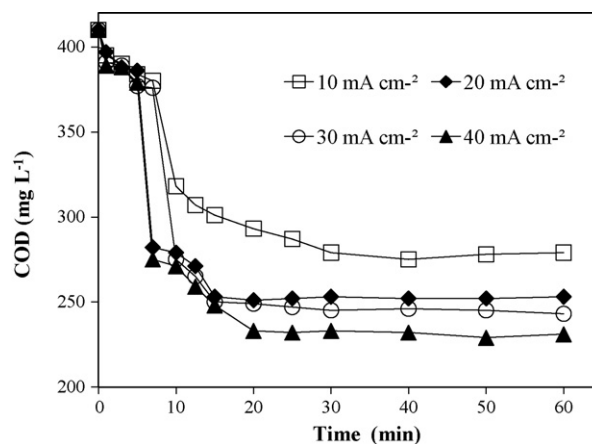


Fig. 3. Reduction of COD ( $\text{mg L}^{-1}$ ) as a function of electrochemical treatment time at current densities of 10, 20, 30, and  $40 \text{ mA cm}^{-2}$  at pH 7.

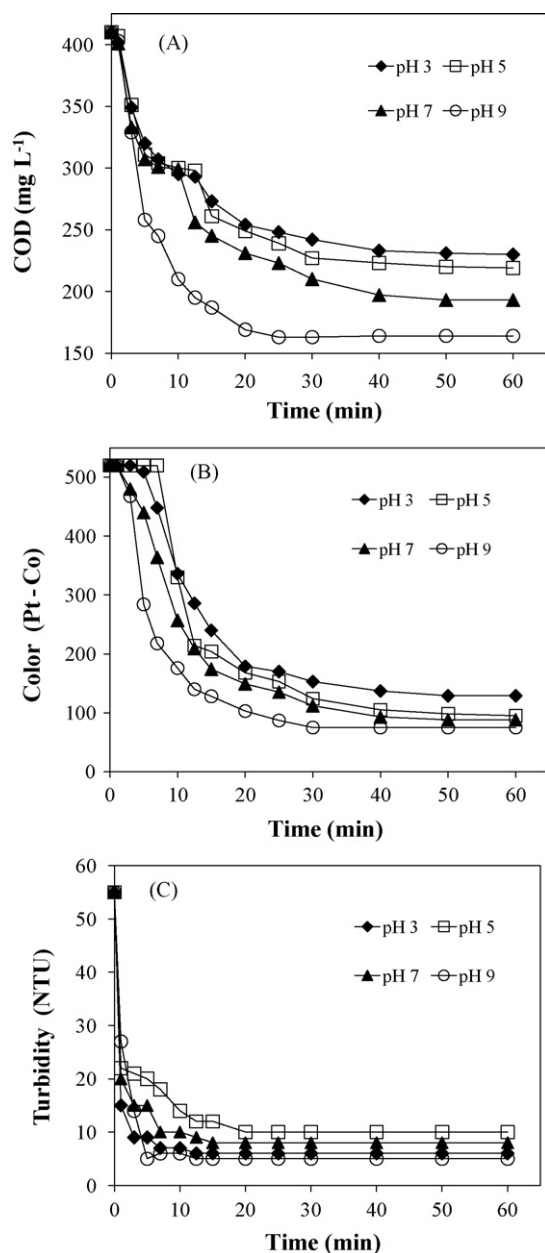


Fig. 4. Reduction of (A) COD (mg L<sup>-1</sup>), (B) color (Pt-Co) and (C) turbidity (NTU) as a function of ozone treatment time at pH 3, 5, 7 and 9.

maceutical, textile, food and chemical). Thus the presence of several compounds and therefore functional groups is expected. According to literature [40,41], the specific rate constants are significantly different for organic and for inorganic compounds. Furthermore, it has been evidenced in such studies that the ozonation rate constant is a function of chain linearity and aromaticity, and that the attack to the latter by ozone is more likely to occur than the attack to the former. Also, it has been reported [40,41] that compounds containing anions from binary and ternary salts (i.e., NO<sub>3</sub><sup>-</sup>, SO<sub>4</sub><sup>-</sup>, and PO<sub>4</sub><sup>-</sup>), amines and melanoidins are unlikely to be mineralized by ozone. Therefore, this type of compounds could be diminishing ozone oxidizing efficiency and then leading to only a partial COD removal. Ozone is a strong oxidant that oxidizes organic pollutants via two pathways: Eq. (5) direct oxidation with ozone molecules and/or the generation of free-radical intermediates (Eqs. (5) and (6)), such as the •OH radical, which is a powerful, effective, and non-selective oxidizing agent [18]. According to Tomiyasu et al. [54], ozonation

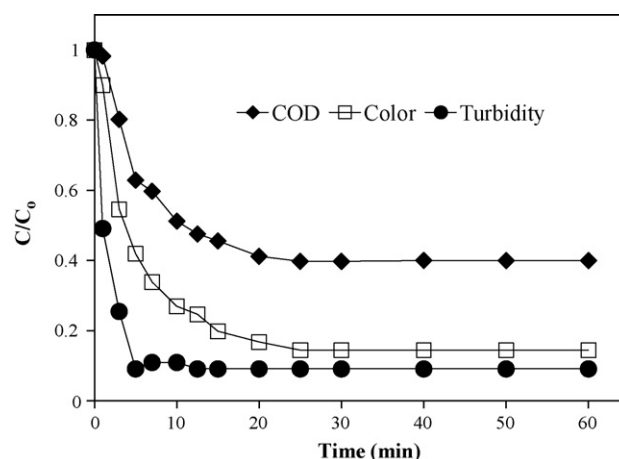
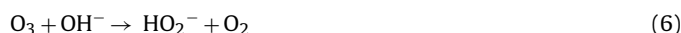


Fig. 5. Effect of COD/COD<sub>0</sub>, Color/Color<sub>0</sub> and Turbidity/Turbidity<sub>0</sub> removal at pH of 9 as a function of ozone treatment time.

may be initiated via one or both of the following equations:

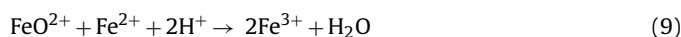
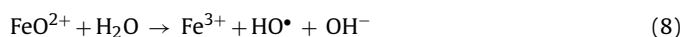


thus the initiation of ozone via OH anions (Eqs. (5) and (6)) may be responsible for the greatest reduction (59%) occurred at pH 9 where a higher initial OH concentration occurs. This percentage removal is significantly higher than those at pH 3 (41%), pH 5 (38%) and pH 7 (34%). Thus, it is evident that ozonation performs best under alkaline conditions, where ozonation initiated via OH anions is also occurring. The color and turbidity as a function of treatment time for different pH values are shown in Fig. 4B and C, respectively. Although the reductions in both are great at pH 9, they are very similar at all pH values. This behavior has been reported and attributed to the ozone reacting with large organic molecules and the formation of carboxylic acids [42–45], which reduces the color and turbidity, but not the COD. The reduction of COD, color, and turbidity as a function of treatment time at pH 9 is shown in Fig. 5. It can be observed, that ozonation only partially reduces COD but almost completely eliminates color and turbidity, which matches similar results by others [46,47]. This confirms (as above suggested) that there are compounds in the complex treated effluent that are recalcitrant to ozone attack and thus their complete mineralization is more difficult to achieve. This fact encourages the coupling of ozonation with other techniques such as electrochemical treatment.

### 3.3. Integrated electrochemical–ozone process system

#### 3.3.1. Effect of pH

pH is a critical parameter in determining the performance of the process. In our experiments, we used pH values of 3, 5, 7 and 9 in the integrated electrochemical–ozone process system. The COD as a function of treatment time for these pH values is shown in Fig. 6A. The maximum COD reduction occurs at pH 7 (88%), but pH 3 (80%) and pH 9 (83%) are also very effective after 20 min reaction time. The hydroxide radicals produced by the ozone under alkaline conditions (Eq. (5)) [18,44] are enhanced by the electrocoagulation produced iron ions (Eqs. (1) and (2)). When ozone is bubbled into an electrochemical system, Fe<sup>2+</sup> catalyzes ozone decomposition to generate hydroxyl radicals as follows [48,49]:



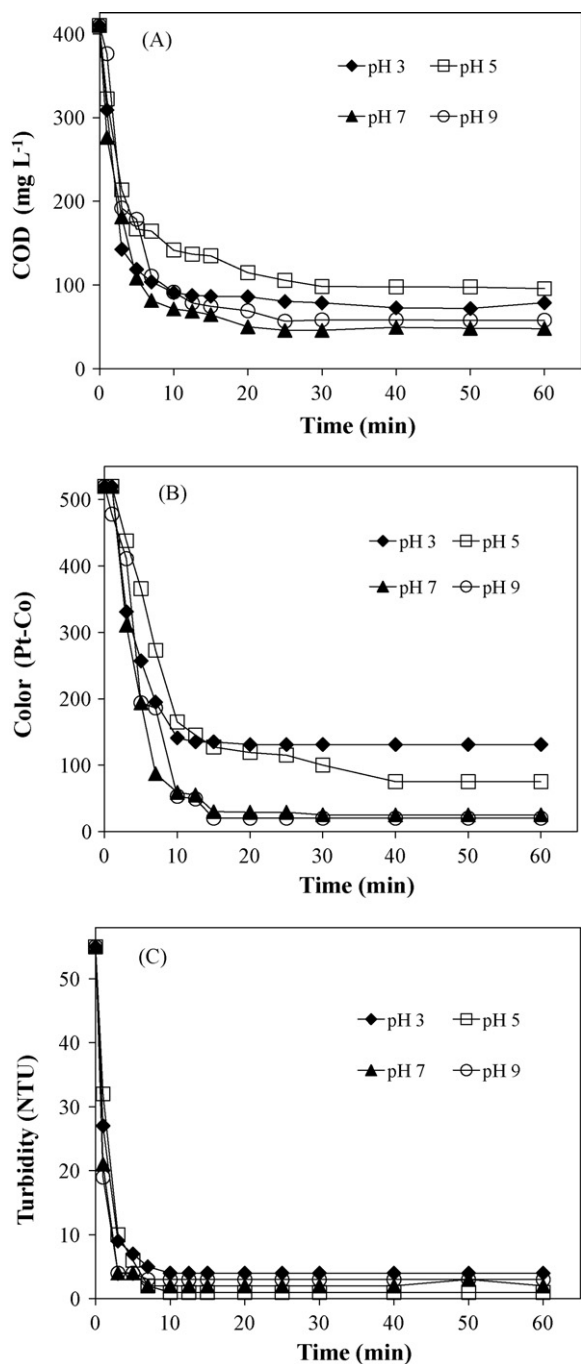


**Fig. 6.** Reduction of (A) COD ( $\text{mg L}^{-1}$ ), (B) color (Pt-Co) and (C) turbidity (NTU) as a function of integrated treatment time at pH 3, 5, 7, and 9 with an applied current density of  $20 \text{ mA cm}^{-2}$ .

The color as a function of time for different pH values is shown in Fig. 6B, the color removal efficiency clearly increased with the increase of pH from 3 to 9. The maximum decolorization of 97% was observed at pH 9.0 after only 15 min of treatment.  $\text{Fe}^{2+}/\text{Fe}^{3+}$  conversion can explain this result: for the iron electrodes at high pH, some of the hydroxide ions may be oxidized at the anode, reducing the production of iron ions. In addition,  $\text{Fe}(\text{OH})_6^{3-}$  or  $\text{Fe}(\text{OH})_4^-$  ions may be present at high pH. These factors lead to reduced color removal efficiency at high pH. Fig. 6C, shows turbidity removal as a function of pH. After 10 min reaction time, the turbidity removal percentage was pH 3 (92%), pH 5 (98%), pH 7 and pH 9 (94%), respectively.

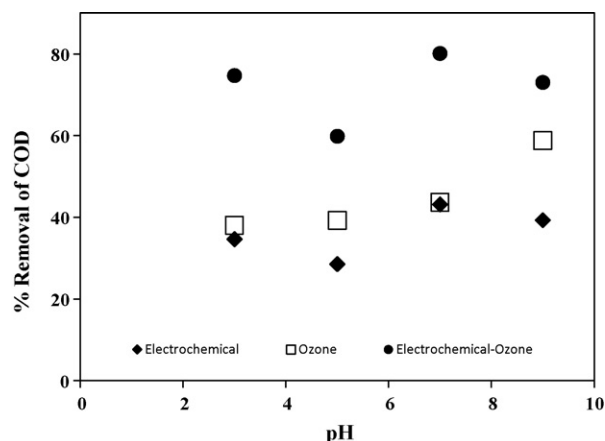


**Fig. 7.** Depicts a comparison of the effect of pH on the COD % removal achieved by the three different treatments (electrochemical, ozonation and integrated electrochemical-ozonation).

Fig. 7 depicts a comparison of the effect of pH on the COD % removal achieved by the three different treatment, i.e., electrochemical, ozonation and integrated electrochemical-ozone. This percentage is the one attained after 20 min of each treatment and applying an electric current of  $20 \text{ mA cm}^{-2}$ . This time was chosen since corresponds to the equilibrium time for at least one of the essayed pH for every treatment. It can be observed that the effect of pH is practically the same in the electrochemical and in the integrated method. Hence it can be said that, although the integrated process involves the production of oxidant species via three routes, electrocoagulation, ozonation and catalytic ozonation, the electrocoagulation remains as the dominant process and is being aided by the catalytic ozonation that provides a higher concentration of  $\text{OH}^-$ . This favors Eq. (3) and monomeric species whose effect has been described earlier in this text. At the same time, a higher  $\text{OH}^-$  concentration favors also the ozonation process. It is worth noticing that for the integrated process neutral pH leads also to highest removal efficiency and since the effluent pH is 7.5 this increases the integrated process sustainability.

### 3.3.2. Influence of applied current density

The COD as a function of time for current densities of 10, 20, 30 and  $40 \text{ mA cm}^{-2}$  at pH 7 is shown in Fig. 8. While  $40 \text{ mA cm}^{-2}$  was higher than 10 and 30 like in the electrocoagulation alone,  $20 \text{ mA cm}^{-2}$  actually had a slightly higher COD reduction than

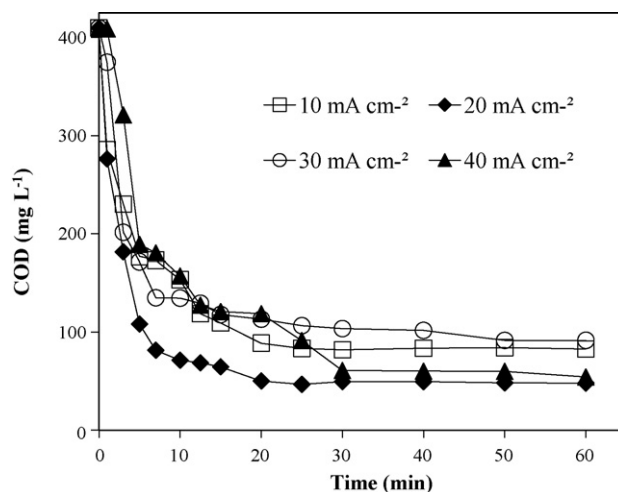


**Fig. 8.** Reduction of COD ( $\text{mg L}^{-1}$ ) as a function of integrated electrochemical-ozone treatment time at current densities of 10, 20, 30, and  $40 \text{ mA cm}^{-2}$ .



**Table 1**  
The characteristics of wastewater industrial treatment plant, treated effluent by electrochemical, ozone and integrated electrochemical–ozone process at 20 min.

Parameters	Wastewater industrial treatment plant	Electrochemical	Ozone	Integrated electrochemical–ozone
COD (mg L <sup>-1</sup> )	410 (±0.49)	233 (±0.49)	163 (±0.49)	65 (±0.49)
BOD <sub>5</sub> (mg L <sup>-1</sup> )	191 (±0.49)	110 (±0.49)	77 (±0.49)	39 (±0.49)
Color (Pt–Co)	520 (±0.49)	63 (±0.49)	30 (±0.49)	25 (±0.49)
Turbidity (NTU)	55 (±0.49)	5 (±0.47)	6 (±0.49)	2 (±0.47)
pH	7.5 (±0.49)	7 (±0.48)	9 (±0.48)	7 (±0.48)
Fecal coliforms, MPN (mg L <sup>-1</sup> )	55,000 (±0.44)	>3 (±0.44)	>1 (±0.46)	>1 (±0.46)
Total solids (mg L <sup>-1</sup> )	4820 (±0.49)	1307 (±0.49)	981 (±0.49)	46 (±0.49)

40. The COD reduction at 10 mA cm<sup>-2</sup> was 71% and at 30 and 40 mA cm<sup>-2</sup> was 69% after 12.5 min of reaction time. Thus, the maximum reduction in COD (87%) was achieved at a current density of 20 mA cm<sup>-2</sup> at pH 7 after 20 min reaction time. Considering the economic factor here, a reasonable current density in our experiments was 20 mA cm<sup>-2</sup>. The variation of the COD, color and turbidity with the integrated electrochemical–ozone process at pH 7 with 20 mA cm<sup>-2</sup> is shown in Fig. 9.

#### 3.4. Optimum conditions applied to wastewater for electrochemical, ozone and integrated electrochemical–ozone process

The physicochemical characteristics of the wastewater from the industrial treatment plant are 410 mg L<sup>-1</sup> of COD, 191 mg L<sup>-1</sup> of BOD<sub>5</sub>, 520 Pt–Co of color, 55 NTU of turbidity, pH 7.5, 55,000 mg L<sup>-1</sup> MPN of fecal coliforms and 4820 mg L<sup>-1</sup> of total solids. The characteristics of the electrochemical, ozone and integrated electrochemical–ozone treated effluent and the overall treatment efficacy are summarized in Table 1. The electrochemical process reduced COD by 43%, BOD<sub>5</sub> by 42%, color by 86%, turbidity by 90%, fecal coliforms by 98%, and total solids by 72%. The ozone process reduced COD by 60%, BOD<sub>5</sub> by 60%, color by 94%, turbidity by 89%, fecal coliforms by 99%, and total solids by 79%. Because of large amounts of flocs formed in the integrated electrochemical–ozone process, the final COD, BOD<sub>5</sub> and fecal coliform reductions reached 84%, 79% and 99%, respectively. Thus, the integrated electrochemical–ozone process improves the effluent in reducing color and turbidity, and especially in enhancing the COD removal.

#### 3.5. Sludge formation in the integrated process

In the electrochemical process the pollutants are removed by the formation of insoluble species as Eq. (4) indicates. However, in the

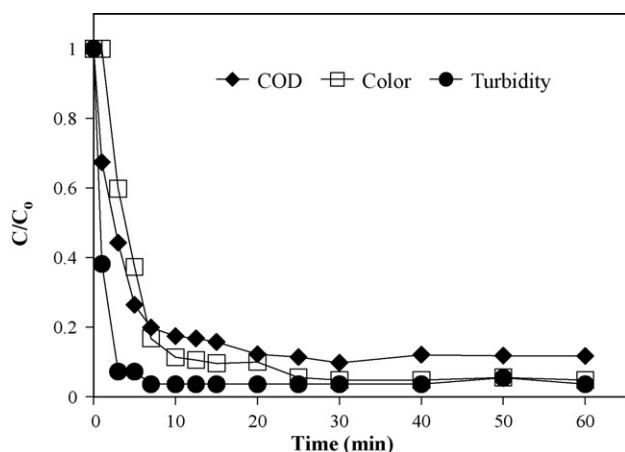


**Fig. 9.** COD/COD<sub>0</sub>, Color/Color<sub>0</sub>, and Turbidity/Turbidity<sub>0</sub> as a function of integrated electrochemical–ozone treatment time at pH 7 with 20 mA cm<sup>-2</sup>.

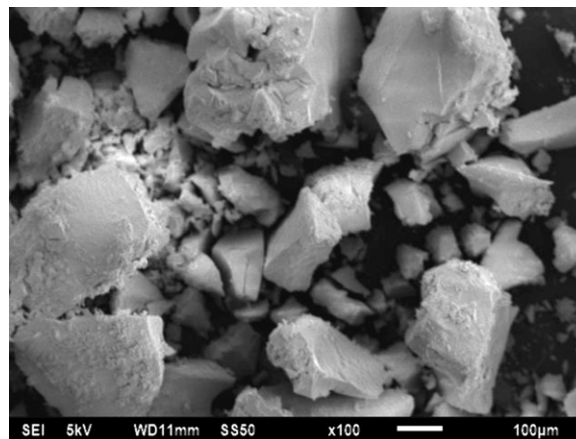


**Fig. 10.** Scanning electron micrographs (×100 magnification) of the sludge generated by integrated electrochemical–ozone process.

integrated process iron ions are produced and interact with ozone as Eqs. (7) and (8) show. Indeed, the amount of sludge generated in the electrochemical process is 250 g L<sup>-1</sup> while in the integrated process is 50 g L<sup>-1</sup>. Although organic matter removal also increased with increasing current density there was not proportionality between the amount of sludge produced and the organic matter removal. Therefore, the dominant mechanism of organic matter removal is likely to be direct oxidation in the present case. The characteristics of the formed chemical sludge were satisfactory, particularly, at the current density of 20 mA cm<sup>-2</sup> for which the amount of dry sludge is 50 g L<sup>-1</sup>. The amount of sludge produced for the integrated electrochemical–ozone is more compact and smaller than that obtained using conventional biological or chemical treatments. The amount of sludge produced compares well with other treatment applications found in the scientific literature [50–53]. SEM provided information about the morphology and composition of the sludge generated by the integrated electrochemical–ozone process. In Fig. 10, it can be observed that the generated sludge appears to be heterogeneous in both, shape and size. By EDX, it was found that the sludge was mainly constituted by iron, carbon and oxygen.

## 4. Conclusions

While ozonation is fast and effective for reducing color and turbidity, it is not so effective at reducing persistent organic compounds and thus, COD in industrial effluents. The effectiveness of COD reduction is greatly enhanced (87% vs. 60%) by coupling ozonation with electrocoagulation. Additionally, the optimum pH is reduced from 9 to 7, bringing it closer to that of the original wastewater. While electrocoagulation efficiency usually increases with increasing current density, the coupled process is more efficient at a relatively low (20 mA cm<sup>-2</sup>) current density.

## Acknowledgments

The authors wish to acknowledge the support given by the Centro Conjunto de Investigación en Química Sustentable, UAEM-UNAM (Project-2794/2009 UAEM) support of CONACYT and supporting research by SNI are greatly appreciated.

## References

- [1] J. Rivas, O. Gimeno, F. Beltrán, Wastewater recycling: application of ozone based treatments to secondary effluents, *Chemosphere* 74 (2009) 854–859.
- [2] D.S.S. Raj, Y. Anjaneyulu, Evaluation of biokinetic parameters for pharmaceutical wastewaters using aerobic oxidation integrated with chemical treatment, *Process Biochem.* 40 (2005) 165–175.
- [3] G. Bertanza, C. Collivignarell, I.R. Pedrazzen, The role of chemical oxidation in combined chemical–physical and biological processes: experience of industrial wastewater treatment, *Water Sci. Technol.* 44 (2001) 109–116.
- [4] M.I. Badawy, R.A. Wahaab, A.S. El-Kalliny, Fenton-biological treatment processes for the removal of some pharmaceuticals from industrial wastewater, *J. Hazard. Mater.* 167 (2009) 567–574.
- [5] A. Gutowska, J. Kauzna-Czapłinska, W.K. Jozwiak, Degradation mechanism of Reactive Orange 113 dye by  $H_2O_2/Fe^{2+}$  and ozone in aqueous solution, *Dyes Pigments* 74 (2007) 41–46.
- [6] C.H. Wu, Decolorization of C.I. Reactive Red 2 in  $O_3$ , Fenton-like and  $O_3$ /Fenton-like hybrid systems, *Dyes Pigments* 76 (2008) 187–194.
- [7] E. Kusvuran, A. Samil, O.M. Atanur, O. Erbatur, Photocatalytic degradation kinetics of di- and tri-substituted phenolic compounds in aqueous solution by  $TiO_2/UV$ , *Appl. Catal.* 58 (B) (2005) 211–216.
- [8] S. Irmak, E. Kusvuran, O. Erbatur, Degradation of 4-chloro-2-methylphenol in aqueous solution by UV irradiation in the presence of titanium dioxide, *Appl. Catal.* 54 (B) (2004) 85–91.
- [9] W.H. Glaze, J.W. Kang, D.H. Chapin, The chemistry of water-treatment processes involving ozone, hydrogen-peroxide and ultraviolet-radiation, *Ozone Sci. Eng.* 9 (1987) 335–352.
- [10] D. Hermosilla, M. Cortijo, C.P. Huang, Optimizing the treatment of landfill leachate by conventional Fenton and photo-Fenton processes, *Sci. Total Environ.* 407 (2009) 3473–3481.
- [11] Y.K. Kim, I.R. Huh, Enhancing biological treatability of landfill leachate by chemical oxidation, *Environ. Eng. Sci.* 14 (1997) 73–79.
- [12] T.A. Kurniawan, W.H. Lo, G.Y.S. Chan, Radicals-catalyzed oxidation reactions for degradation of recalcitrant compounds from landfill leachate, *Chem. Eng. J.* 125 (2006) 35–57.
- [13] S.A. Parsons, *Advanced Oxidation Processes for Water and Wastewater Treatment*, IWA Publishing, London, 2004.
- [14] R. Rosal, A. Rodríguez, J.A. Perdigón-Melón, A. Petre, E. García-Calvo, Oxidation of dissolved organic matter in the effluent of a sewage treatment plant using ozone combined with hydrogen peroxide ( $O_3/H_2O_2$ ), *Chem. Eng. J.* 149 (2009) 311–318.
- [15] B.H. Lee, W.C. Song, B. Manna, J.K. Ha, Dissolved ozone flotation (DOF) a promising technology in municipal wastewater treatment, *Desalination* 225 (2008) 260–273.
- [16] T.A. Larsen, J. Lienert, A. Joss, H. Siegrist, How to avoid pharmaceuticals in the aquatic environment, *J. Biotechnol.* 113 (2004) 295–304.
- [17] S. Esplugas, J. Giménez, S. Contreras, E. Pascual, M. Rodríguez, Comparison of different advanced oxidation processes for phenol degradation, *Water Res.* 36 (2002) 1034–1042.
- [18] S. Song, J. Yao, Z. He, J. Qiu, J. Chen, Effect of operational parameters on the decolorization of C.I. Reactive Blue 19 in aqueous solution by ozone-enhanced electrocoagulation, *J. Hazard. Mater.* 152 (2008) 204–210.
- [19] P.C.C. Faria, J.J.M. Orfão, M.F.R. Pereira, Activated carbon catalytic ozonation of oxamic and oxalic acids, *Appl. Catal. B: Environ.* 79 (2008) 237–243.
- [20] N. Burns, G. Hunter, A. Jackman, B. Hulse, J. Coughenour, T. Walz, The return of ozone and the hydroxyl radical to wastewater disinfection, *Ozone Sci. Eng.* 29 (2007) 303–306.
- [21] K. Ikehata, N.J. Naghashkar, M.G. El-Din, Degradation of aqueous pharmaceuticals by ozonation and advanced ozonation processes: a review, *Ozone Sci. Eng.* 28 (2006) 353–414.
- [22] P.R. Gogate, A.B. Pandit, A review of imperative technologies for wastewater treatment, I. Oxidation technologies at ambient conditions, *Adv. Environ. Res.* 8 (2004) 501–551.
- [23] P.R. Gogate, A.B. Pandit, A review of imperative technologies for wastewater treatment, II. Hybrid methods, *Adv. Environ. Res.* 8 (2004) 553–597.
- [24] P.K. Holt, G.W. Barton, C.A. Mitchell, A quantitative comparison between chemical dosing and electrocoagulation, *Colloids Surf.* 11 (A2) (2002) 233–248.
- [25] P. Holt, G. Barton, A. Mitchell, Deciphering the science behind electrocoagulation to remove suspended clay particles from water, *Water Sci. Technol.* 50 (2004) 177–184.
- [26] E. Kusvuran, O. Gulnaz, A. Samil, M. Erbil, Detection of double bond-ozone stoichiometry by an iodimetric method during ozonation processes, *J. Hazard. Mater.* 175 (2010) 410–416.
- [27] Standard Methods for the Examination of Water and Wastewater Procedures (APHA, AWWA and WPCF), 1989.
- [28] A.K. Golder, N. Hridaya, A.N. Samanta, S. Ray, Electrocoagulation of methylene blue and eosin yellowish using mild steel electrodes, *J. Hazard. Mater.* 127 (B) (2005) 134–140.
- [29] W. Chung-Hsin, C. Chung-Liang, K. Chao-Yin, Decolorization of Procion Red MX-5B in electrocoagulation (EC), UV/ $TiO_2$  and ozone-related systems, *Dyes Pigments* 76 (2008) 187–194.
- [30] M.Y.A. Mollah, R. Schennach, J.R. Parga, D.L. Cocke, Electrocoagulation science and applications, *J. Hazard. Mater.* 84 (2001) 29–41.
- [31] J.G. Ibanez, M.M. Singh, Z. Szafran, Laboratory experiments on electrochemical remediation of the environment. Part 4. Color removal of simulated wastewater by electrocoagulation–electroflotation, *J. Chem. Educ.* 75 (1998) 1040–1041.
- [32] N. Daneshvar, A. Oladegaragoze, N. Djafarzadeh, The use of artificial neural networks (ANN) for modeling of decolorization of textile dye solution containing C.I. Basic Yellow 28 by electrocoagulation process, *J. Hazard. Mater.* B129 (2006) 116–122.
- [33] N. Daneshvar, A.R. Khataee, G.A.R. Amani, M.H. Rasoulifard, Decolorization of C.I. Acid Yellow 23 solution by electrocoagulation process: investigation of operational parameters and evaluation of specific electrical energy consumption (SEEC), *J. Hazard. Mater.* 148 (2007) 566–572.
- [34] P. Cañizares, C. Jiménez, F. Martínez, C. Saez, M.A. Rodrigo, Study of the electrocoagulation process using aluminum and iron electrodes, *Ind. Eng. Chem. Res.* 46 (2007) 6189–6195.
- [35] A.F. Martínez, M.L. Wilde, T.G. Vasconcelos, D.M. Henriques, Nonylphenol polyethoxylate degradation by means of electrocoagulation and electrochemical Fenton, *Sep. Purif. Technol.* 50 (2) (2006) 249–255.
- [36] H.C.A. Martínez, E. Brillas, Decontamination of wastewaters containing synthetic organic dyes by electrochemical methods, *Appl. Catal. B: Environ.* 87 (2009) 105–145.
- [37] M. Panizza, G. Cerisola, Electrochemical materials for the electrochemical oxidation of synthetic dyes, *Appl. Catal. B: Environ.* 75 (2007) 95–101.
- [38] M. Panizza, G. Cerisola, Electrochemical degradation of methyl red using BDD and  $PbO_2$  anodes, *Ind. Eng. Chem. Res.* 47 (2008) 6816–6820.
- [39] M. Bayramoglu, M. Kobya, O.T. Can, M. Sozbir, Operating cost analysis of electrocoagulation of textile dye waste water, *Sep. Purif. Technol.* 37 (2004) 117–125.
- [40] T. Sreethawong, S. Chavadej, Color removal of distillery wastewater by ozonation in the absence and presence of immobilized iron oxide catalyst, *J. Hazard. Mater.* 155 (2008) 486–493.
- [41] J. Hoigne, H. Bader, Rate constants of reactions of ozone with organic and inorganic compound in water-I, *Water Res.* 17 (1983) 173–183.
- [42] J. Hoigne, H. Bader, The role of hydroxyl radical reactions in ozonation processes in aqueous solutions, *Water Res.* 10 (1976) 377–386.
- [43] B. Yan-Lan, R. Nigmatullin, G. Li-Puma, Ozonation kinetics of cork-processing water in a bubble column reactor, *Water Res.* 42 (2008) 2473–2482.
- [44] H.Y. Shu, C.R. Huang, Degradation of commercial azo dyes in water using ozonation and UV enhanced ozonation process, *Chemosphere* 31 (8) (1995) 3813–3825.
- [45] O.S.G.P. Soares, J.J.M. Orfão, D. Portela, A. Vieira, M.F.R. Pereira, Ozonation of textile effluents and dye solutions under continuous operation: influence of operating parameters, *J. Hazard. Mater.* 3 (B 137) (2006) 1664–1673.
- [46] M.H.P. Santana, L.M. Da Silva, A.C. Freitas, J.F.C. Boodts, K.C. Fernandes, L.A. De Faria, Application of electrochemically generated ozone to the discoloration and degradation of solutions containing the dye Reactive Orange 122, *J. Hazard. Mater.* 164 (2009) 10–17.
- [47] K. Chun-Han, H. Po-Hung, C. Meng-Wen, C. Jia-Ming, C. Shih-Min, T. Chewn-Jeng, Kinetics of pulp mill effluent treatment by ozone-based processes, *J. Hazard. Mater.* 168 (2009) 875–881.
- [48] B. Legube, N. Kerpel Vel Leitner, Catalytic ozonation: a promising advanced oxidation technology for water treatment, *Catal. Today* 53 (1999) 61–72.
- [49] H.B. Kasprzyk, M. Ziolk, J. Nawrocki, Catalytic ozonation and methods of enhancing molecular ozone reactions in water treatment, *Appl. Catal. B: Environ.* 46 (2003) 639–669.
- [50] I. Arslan-Alaton, I. Kabdas, B. Vardar, O. Tünay, Electrocoagulation of simulated reactive dyebath effluent with aluminum and stainless steel electrodes, *J. Hazard. Mater.* 164 (2009) 1586–1594.
- [51] I. Kabdas, B. Vardar, I. Arslan-Alaton, O. Tünay, Effect of dye auxiliaries on color and COD removal from simulated reactive dyebath effluent by electrocoagulation, *Chem. Eng. J.* 148 (2009) 89–96.
- [52] I. Kabdas, I. Arslan-Alaton, B. Vardar, O. Tünay, Comparison of electrocoagulation, coagulation and the Fenton process for the treatment of reactive dyebath effluent, *Water Sci. Technol.* 55 (2007) 125–136.
- [53] I. Kabdas, T. Arslan, T. Ölmez-Hanci, I. Arslan-Alaton, O. Tünay, Complexing agent and heavy metal removals from metal plating effluent by electrocoagulation with stainless steel electrodes, *J. Hazard. Mater.* 165 (2009) 838–845.
- [54] H. Tomiyasu, H. Fukutomi, G. Gordon, Kinetics and mechanism of ozone decomposition in basic aqueous solution, *Inorg. Chem.* 24 (1985) 2962–2966.